Current Research in Insect Science 2 (2022) 100033

Contents lists available at ScienceDirect

Current Research in Insect Science

journal homepage: www.elsevier.com/locate/cris

Research article

Engineering of Cry3Bb1 provides mechanistic insights toward countering western corn rootworm resistance

Suyog S. Kuwar[a], Ruchir Mishra[a], Rahul Banerjee[a], Jason Milligan[b], Timothy Rydel[b], Zijin Du[b], Zhidong Xie[b], Sergey Ivashuta[b], Jean-Louis Kouadio[b], Jason M. Meyer[b], Bryony C. Bonning[a,*]

[a] Department of Entomology and Nematology, University of Florida, Gainesville, FL, USA
[b] Bayer U.S., Research and Development, Crop Science Plant Biotechnology, Chesterfield, MO, 63017 USA

ARTICLE INFO

Keywords:
western corn rootworm
resistance
Cry3Bb1
phage display
gut binding peptide

ABSTRACT

The western corn rootworm (WCR), *Diabrotica virgifera virgifera* LeConte (Coleoptera: Chrysomelidae), is an economically important pest of corn (maize) in North America and Europe. Current management practices for WCR involve transgenic expression of insecticidal proteins to minimize larval feeding damage to corn roots. The evolution of resistant WCR populations to transgenic corn expressing insecticidal proteins (e.g. Cry3Bb1, Gpp34Ab1/Tpp35Ab1) necessitates efforts to discover and deploy new modes of action for WCR control. Here, we tested the hypothesis that the addition of short peptides selected for binding to the WCR gut would restore insecticidal activity of Cry3Bb1 to resistant insects. Phage display technology coupled with deep sequencing was used to identify peptides selected for binding to WCR brush border membrane vesicles and to recombinant putative receptors aminopeptidase and cadherin. The binding and specificity of selected peptides was confirmed by ELISA and pull-down assays, and candidate gut surface binding partners were identified. Although production of 284 novel Cry3Bb1 variants with these peptides did not restore activity against resistant WCR in artificial diet bioassays, 112 variants were active against susceptible insects. These results provided insights for the mechanism of Cry3Bb1 activity and toward engineering a new mode-of-action via receptor re-targeting in the context of protein structure and function.

1. Introduction

The western corn rootworm (WCR), *Diabrotica virgifera virgifera* LeConte (Coleoptera: Chrysomelidae), is a damaging pest of maize (Krysan and Miller 1986). It is the most devastating corn pest in both North America (Gray et al. 2008) and in Europe (Lombaert et al. 2018). Larval feeding on root tissue can disrupt water and nutrient uptake and undermine structural support, thus increasing susceptibility to damage from rain and wind events (Urías-López and Meinke 2001; Tinsley, Estes, and Gray 2013). Adult WCR feed on maize silk during pollen shed which can cause poorly filled ears (Krysan and Miller 1986). The impact of WCR extends to ~30 million acres of corn in the U.S. at an estimated cost of >$1 billion annually (Wechsler and Smith 2018).

Integrated pest management of WCR includes the use of insecticides, crop rotation, and transgenic varieties that express *Bacillus thuringiensis* (Bt)-derived pesticidal proteins (Ball and Weekman 1963; Zukoff et al. 2016). Current biotech traits available for WCR control include Gpp34Ab1/Tpp35Ab1 (formerly Cry34Ab1/ Cry35Ab1 (Crickmore et al. 2021)), Cry3Bb1, mCry3A, and eCry3.1Ab (Walters et al. 2008; Walters et al. 2010; Kelker et al. 2014; Moellenbeck et al. 2001; Vaughn et al. 2005). Field populations of WCR have evolved resistance to these control measures (Meihls et al. 2008; Petzold-Maxwell et al. 2012; Gassmann et al. 2014; Gassmann et al. 2011; Gray 2012; Schrader et al. 2017; Zukoff et al. 2016; Gassmann et al. 2020), making sustainable management challenging (Ball and Weekman 1963; Zukoff et al. 2016). Moreover, the expansion of WCR host plants suggested or confirmed for soybean, oil pumpkin and *Miscanthus* grass (Meinke et al. 2009; Spencer and Raghu 2009) complicates our understanding of the distribution of WCR populations.

Relatively little is known about the mode of action of Cry3Bb1 or the WCR gut surface receptors that mediate the insecticidal properties. While resistance to Cry3Bb1 (>50-fold, which extends to mCry3A and eCry3.1Ab) in the lab-based colony used in this study (Moar et al. 2017) was mapped to a single locus on chromosome 8, other resistance loci, or modifiers of resistance are also implicated (Flagel et al. 2015; Willse, Flagel, and Head 2021). This region of the chromosome contains the gene encoding the ATP-binding cassette (ABC) transporter, ABCB2. ABCB1, which has 67% amino acid identity to ABCB2, has been implicated in mCry3A resistance in WCR (Niu et al. 2020) and

* Corresponding author: Department of Entomology and Nematology, University of Florida, PO Box 110620, Gainesville, FL 32611.
E-mail address: bbonning@ufl.edu (B.C. Bonning).

https://doi.org/10.1016/j.cris.2022.100033
Received 4 November 2021; Received in revised form 21 February 2022; Accepted 23 February 2022

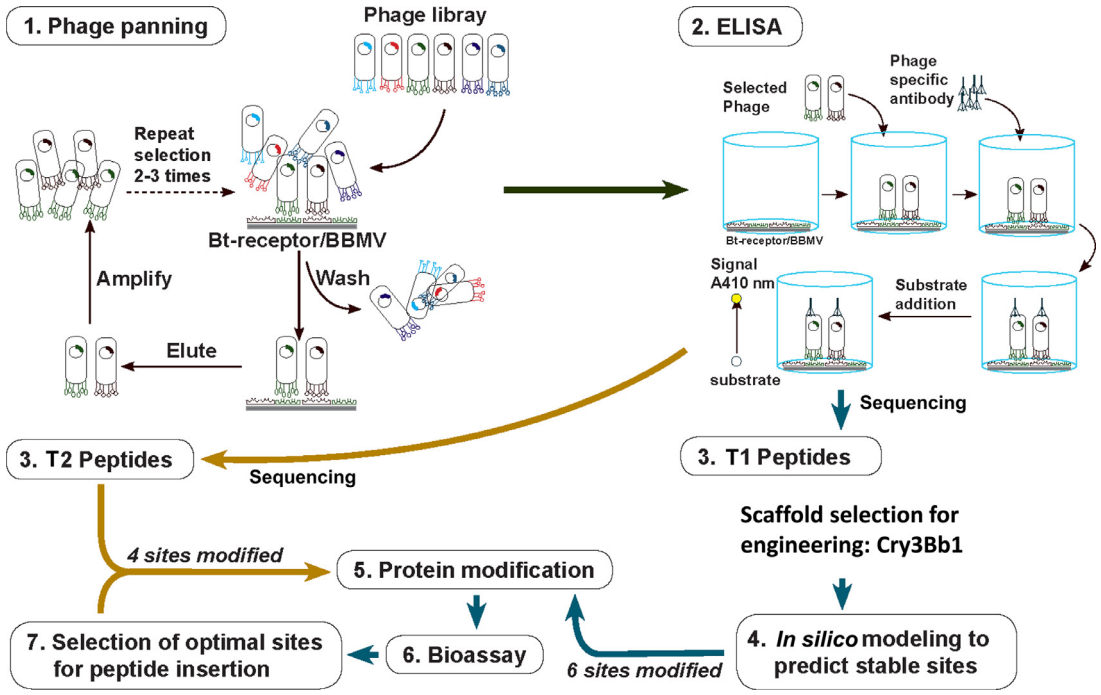

Figure 1. Workflow for protein engineering process in this study.

in Cry3Aa resistance in another coleopteran pest (Pauchet et al. 2016). An RNAi screen of ABC transporters in *Tribolium castaneum* showed that silencing of TcABCB-3B, the WCR ABCB1 homolog, had no phenotypic effect suggesting that this protein is not essential for survival in Coleoptera and that there is redundancy in ABC transporter function (Broehan et al. 2013). In addition to ABC transporter proteins, cadherin-like proteins have been implicated in other coleopteran species as putative receptors for Cry3Aa, Cry3Ba, and Cry3Bb (Fabrick et al. 2009; Hua, Park, and Adang 2014; Park et al. 2009; Park et al. 2019; Contreras et al. 2013), and aminopeptidase N (APN) has been noted as a receptor for other three-domain Cry proteins (Zhang, Hua, and Adang 2017; Guo et al. 2020). As cadherin and APN are both expected to be abundant on the surface of the WCR gut epithelium, these proteins were of particular interest for the current study.

New modes-of-action for WCR control could mitigate the effects of emerging resistance to existing and forthcoming management tools and practices. Next-generation gene-stacks have been developed that combine previously deployed Bt –derived pesticidal proteins with a new trait for WCR control featuring RNA interference (RNAi) technology (Baum et al. 2007; Price and Gatehouse 2008). In addition, removal of the alpha helix of Cry1A and phage-assisted evolution have both been successfully employed to overcome resistance mediated by cadherin in Lepidoptera (Badran et al. 2016; Soberon et al. 2007).

In this study, we combined phage display technology with rational protein design to engineer novel Cry3Bb1 variants; our goals were to gain understanding regarding relationships between structure and function toward ultimately restoring activity against Cry3Bb1-resistant WCR. If successful, this approach could enable repurposing of Cry3Bb1 to extend WCR control via transgenic expression in corn. The Cry3Bb1 protein scaffold was modified with new peptides that specifically bind 1) WCR brush border membrane vesicles (BBMV), for which candidate binding partners on the surface of the gut epithelium were identified, or 2) the recombinant putative Cry3Bb1 receptors APN and cadherin (CAD). Results from the initial, Tier-1 peptide-modified Cry3Bb1 (four peptides; six insertion regions) that utilized a tiling-engineering strategy provided a framework for a more sequence-diverse but site-targeted engineering effort in Tier-2 (73 peptides, four insertion regions), based on suitability of positions for engineering relative to insecticidal activity (Fig. 1). Structure-function relationships of the engineered variants relative to performance in artificial diet bioassays for WCR larvae were assessed and used to build our understanding of new variant activity in susceptible vs. inactivity in resistant insect colonies.

2. Materials and Methods

2.1. Targets for phage display

2.1.1. Brush border membrane vesicles

Brush border membrane vesicles (BBMV) were isolated from 3rd instar larvae from Cry3Bb1-susceptible WCR (s-WCR; the BrookS colony) and -resistant WCR (r-WCR; the HopR- also known as the Gass-R-colony) reared on corn roots as previously described (Moar et al. 2017; Flagel et al. 2015; Willse, Flagel, and Head 2021). Preparation of BBMV included selective divalent-cation precipitation and differential centrifugation of BBMV in ice-cold MET buffer (0.3 M mannitol with 5 mM EGTA and 20 mM Tris/HCl at pH 7.5 (Silva-Filha, Nielsen-Leroux, and Charles 1997)). Finally, BBMV were resuspended in MET buffer and stored at -80 ºC until use. Leucine-aminopeptidase assays were conducted on crude homogenates compared to an equal protein concentration of BBMV to assess enrichment of enzymatic activity (Bradford 1976). Assays contained L-leucin-*p*-nitroanilide in 25 mM Tris-HCl buffer (pH 7.5) incubated at 37 ºC for 2.5 hr. Optical density was recorded by a plate reader at 450 nm (Molecular Devices; San Jose, CA) to track *p*-nitroanilide release relative to a negative control.

2.1.2. Recombinant receptors

Amino acid sequences for the receptors used in this study are provided in the supplementary information (Table S1). WCR APN was 100% identical to a 934 amino acid aminopeptidase N-like protein from *D. virgifera virgifera* (GenBank Accession XP_028140411) with the following modifications: a flag tag "DYKDDDDK" was positioned near the N-terminus, following the first 15 amino acids of the protein, and 24 amino acids were truncated from the C-terminus to remove a putative GPI-anchor site predicted by PredGPI (Pierleoni, Martelli, and Casadio 2008). WCR CAD was 99.8% and 99.6% identical to the 1688 amino acid proteins cadherin-23-like protein and cadherin-like protein from *D.*

virgifera virgifera, respectively (NCBI Accession Nos.: XP_028128868.1; AAV88529.2) (Sayed et al. 2007) and included the sequence "GHHHHHH" at the C-terminus. Recombinant proteins were expressed using a standard baculovirus and insect cell expression approach with the Gateway pDEST 8 vector (ThermoFisher Scientific, Waltham, MA) and *flash*BAC™ one-step baculovirus protein expression systems (Oxford Expression Technologies; Oxford, United Kingdom). Proteins were His-tag-purified from Sf9/Sf21 (small-scale) or High Five™ cells (large-scale) using standard procedures. Recombinant receptors were detected by western blot with an anti-His primary antibody (1:3000), secondary antibody conjugated to horseradish peroxidase (1:5000, Molecular Probes; Eugene, OR) with detection using West Pico enhanced chemiluminescence reagent (Thermo Fisher Scientific; Waltham, MA).

2.2. Phage display

Ph.D.™-C7C and Ph.D.™-12 Phage Display Peptide Library Kits (New England Biolabs; Ipswich, MA) were used for biopanning with direct target coating according to the manufacturer's instructions. Individual phage plaques were isolated to provide a snapshot of putative binding peptides by Sanger sequencing for screens against selected targets. Phage pools from rounds 2 and 3 of panning were used for MiSeq™ to deep-sequence eluted phages containing putative binding sequences. DNA was isolated from amplified phage pools using phenol/chloroform extraction followed by chloroform extraction and ethanol precipitation. Phage peptide inserts were amplified for sequencing by an initial polymerase chain reaction (PCR) according to the Platinum™ Taq DNA Polymerase kit (Thermo Fisher Scientific; Waltham, MA) featuring Illumina adaptor extension primers (F-TCGTCGGCAGCGTCAGATGTGTATAAGAGACAG and R-GTCTCGTGGGCTCGGAGATGTGTATAAGAGACAG) and included less than 15 amplification cycles. PCR products were purified using 1X AMPure beads (Beckman Coulter; Brea, CA) according to the directions provided and resuspended in 20ul 10mM Tris (pH8.0) elution buffer. A second PCR was conducted using initial PCR products as the DNA templates with the KAPA HiFi HotStart Library Amp Kit (Roche Sequencing and Life Science, Wilmington, MA) in order to attach Illumina sequencing and barcoding adaptors (T5-AATGATACGGCGACCACCGAGATCTACAC(XXXXXXXX)TCGTCGGCAG CGTCAGATGTGTATAAGAGACAG and T7-CAAGCAGAAGACGGCATAC GAGAT(XXXXXXXX)GTCTCGTGGGCTCGGAGATGTGTATAAGAGACAG (X's=8-mer barcodes) in less than 10 cycles. PCR products were purified as described previously in 25 μl elution buffer. One microliter of each sample was loaded onto an Agilent 2100 Bioanalyzer System (Agilent; Santa Clara, CA) as a quality control to assess size of amplification products and DNA concentration. Samples were then evenly pooled and adjusted for concentration according to the requirements of the MiSeq™ System (Illumina; San Diego, CA) for 2x150 base paired-end sequencing. The resultant sequences were processed to remove adaptor sequences, eliminate low quality reads and deconvolute multiplexing.

2.3. Validation of peptide binders

2.3.1. ELISA (Enzyme-linked immunosorbent assay)

ELISA was used as a screen to validate binding of individual phage clones isolated for Sanger sequencing according to the phage display kit directions (Fig. 1). Plates were directly coated with phage display target material, and uncoated wells were used as negative controls in the assay. Assays using plates coated with BBMV were conducted with s-WCR BBMV due to greater availability of that reagent relative to r-WCR BBMV.

2.3.2. Production of peptide-mCherry fusion proteins

Binding studies were conducted using selected peptide-mCherry fusion proteins. Expression constructs in pBAD/His B (Invitrogen; Carlsbad, CA) were prepared as described previously (Liu et al. 2010) using the linker "GSGSGS". Protein induction was carried out at room temperature (RT) overnight by adding 0.02% L-arabinose. His-tagged fusion proteins were purified using Ni-affinity columns (Capturem Maxiprep kit, Takara) according to the manufacturer's directions. Purification was conducted under native conditions using a batch purification method at 4 °C. Purified protein fractions were separated by SDS-PAGE and stained with Coomassie Brilliant Blue. Protein concentration was determined using the Bradford assay relative to a bovine serum albumin (BSA) standard. Fusion proteins were stored at −80 °C until use.

2.3.3. Pull-down assays

Pull-down binding assays were carried out to investigate the relative and specific binding of peptide-mCherry fusions to s-WCR BBMV as described previously (Chougule et al. 2013). Equal concentrations of s-WCR BBMV protein (5 μg) and 10 nM of peptide-mCherry fusions were co-incubated with 100 nM or 1000 nM of the same peptide but labelled with biotin (Genemed Synthesis Inc. San Antonio, TX) in 100 μl of binding buffer (PBS: 0.1% w/v BSA, 0.1% v/v Tween 20, pH 7.6) for 1 hr. BBMV and any bound proteins were pelleted by centrifugation at 20,000 g for 10 min at 4 °C, and then washed twice by pipetting to remove residual, unbound protein. The final pellet was boiled in 10 μl of SDS-sample buffer for 5 min and centrifuged briefly, and proteins in the supernatant were separated by SDS-PAGE (10% w/v). Proteins were transferred to a nitrocellulose membrane for western blot detection of BBMV-bound peptide-mCherry with anti-mCherry antibodies (Novus Biologicals, Littleton, CO) at a 1:5000 dilution for 1 hour. Antibody binding was detected with the West – Pico Chemioluminescent kit (Thermo Fisher Scientific; Waltham, MA) on exposure to film. Western blot images were processed using ImageJ to estimate the relative amount of peptide-mCherry bound to s-WCR BBMV.

2.3.4. UV-crosslinking assays to identify peptide binding partners

Selected peptides were also assessed for binding using a UV-crosslinking and pull-down assay as described previously (Chougule et al. 2013; Becker and Naider 2015). A total of 270-400 micrograms of BBMV was incubated with p-benzyol-l-phenylalanine (Bpa)-containing peptides for each of five peptides at 50 μg/ml in buffer (MET pH 7.5, 0.1% BSA, 1x-protease inhibitor cocktail and 1 mM PMSF) for 1 h at 4 °C with gentle rotation. Aliquots of 250 μl/well were transferred into chilled 24-well plastic culture plates pre-blocked with MET buffer (pH 7.5, 0.1% BSA). Reactions were divided to maintain a minimal sample depth to permit efficient UV penetration. Samples were held at RT and irradiated without culture plate lids at 365 nm for 1 h at a distance of ~12 cm in a Spectroline Model CM-10A (MilliporeSigma; Burlington, MA). Samples were collected and washed twice by centrifugation at 16,000 g for 15 min with 1xTBS (pH 7, 0.1% BSA). Pellets were solubilized in 50 mM Tris pH 7.5, 150 mM NaCl, 1% SDS at 70 °C for 20 min shaking at 300 rpm. Samples were diluted 2-fold in 50 mM Tris pH 7.5, 150 mM NaCl to reach a final SDS concentration of 0.5%. Ten μl samples were collected for western blot, and the rest of solubilized samples were incubated with 100 μl NeutrAvidin or Streptavidin agarose beads and washed 3 times in TBSS buffer (50 mM Tris pH 7.5, 150 mM NaCl, 0.5% SDS) and 3 times with ultra-pure water. Forty μl of 4xSDS sample loading buffer was added to the beads and incubated at 95 °C for 10 min. Supernatants were loaded on 4-12% Bis-Tris gels (Invitrogen; Carlsbad, CA). BBMV without peptide and BBMV with peptide but without UV exposure were used as negative controls.

Excised gel bands of interest were sent to the Interdisciplinary Center for Biotechnology Research (ICBR, University of Florida) for liquid chromatography with tandem mass spectrometry (LC-MS/MS). Bands from the gel were de-stained with 1 ml 50 mM ammonium bicarbonate pH 8.0/acetonitrile (1:1, v/v). Samples were reduced with 20 mM dithiothreitol (DTT), alkylated with 40 mM of 2-chloroacetamide, and trypsin-digested. Tryptic digested peptides were desalted with C18-Ziptip (MilliporeSigma; Burlington, MA). Gel fractions were run for 90

min on an Orbitrap-Fusion Mass Spectrometer. Peak lists generated from raw tandem mass spectra were searched using Proteome Discoverer 2.2 at the ICBR. Searches were performed against a target database created using protein sequences from beetles belonging to the families Chrysomelidae, Cerambycidae and Curculionidae available at the National Center for Biotechnology Information (NCBI). Further processing of mass spectrometry data was performed using an in-house R Tidyverse package. In brief, proteins with ≥ 2 unique peptides, peptide spectral matches (PSMs) ≥ 2, SequestHT score ≥ 6, predicted to localize to the plasma membrane or have a GPI anchor and unique to the UV crosslinked sample, or ≥ 2-fold the number of peptide spectra in the non-UV crosslinked lane (Gubbens et al. 2009) were considered to be candidate peptide binding partners. Bioinformatics programs PredGPI, Cello2GO and PSORT II, and Phobius were used to predict the presence of a GPI anchor, protein localization, and signal peptide and transmembrane domain, respectively (Pierleoni, Martelli, and Casadio 2008; Yu et al. 2014; Kall, Krogh, and Sonnhammer 2007).

2.4. Cry3Bb1 engineering

2.4.1. Peptide selection

Peptide selection for engineering was based on several criteria including relative: 1) performance in ELISA assays, 2) abundance from MiSeq read counts obtained in round 3 phage pool sequencing, or 3) enrichment determined by comparing MiSeq abundance from read counts per sequence from round 3 versus round 2 of biopanning, 4) binding assessments, and 5) multiple computational analyses, as follows. Select peptides from library screens were queried against MimoDB (Huang et al. 2012). The SAROTUP suite of tests was used to exclude peptides resulting from propagational bias and selection-related false positives (He et al. 2019; Huang et al. 2012). R-studio's Peptide package was used to calculate GRAVY (Grand Average of Hydropathy) score (Kyte and Doolittle 1982) and stability index for peptides that passed the SAROTUP analysis. To find common motifs among the candidate peptides, Multiple Em for Motif Elicitation (MEME) analysis was conducted to identify novel, ungapped motifs (recurring, fixed-length patterns) in sequences using the online MEME software Suite 5.0.2 (http://meme-suite.org/).

2.4.2. Production of peptide-modified Cry3Bb1 variants

Two rounds of Cry3Bb1 variant design and diet bioassay testing were conducted. The rationale for the first round of variants based on peptides selected from Sanger sequencing (Tier 1) was to generate data on the suitability of sites chosen for insertion of Ph.D.™-C7C and Ph.D.™-12 derived peptides for producing constructs active against Cry3Bb1 s-WCR. A subset of these sites selected based on the performance of Tier 1 peptide-modified variants, was then used in production of Tier 2 Cry3Bb1 variants.

Novel Cry3Bb1 designs were created using selected peptide binding sequences as insertions or C-terminal fusions to the Cry3Bb1 scaffold (File S1; Fig. 2). Direct addition of binding peptide to existing sequence (without any corresponding deletion) as previously described (Chougule et al. 2013), was not employed on the basis that this strategy was more likely to disrupt protein structure than replacement of existing amino acid sequences. Engineering sites were chosen based on potential receptor binding regions of the pesticidal protein. Cry3Bb1 structural information was visualized in PyMOL(TM) 2.3.3 (Schrodinger, LLC; pymol.org) (Fig. 2). Based on structural considerations, only 12-mer amino acid peptides (derived from Ph.D.™-12) were inserted into the DII strand/turn site, while both 12-mer amino acid and 7-mer amino acid (Ph.D.™-C7C) peptides were used in the DIII strand/turn. In order to introduce added flexibility, single or double glycine residues flanking peptide insertions were included in some cases (File S1).

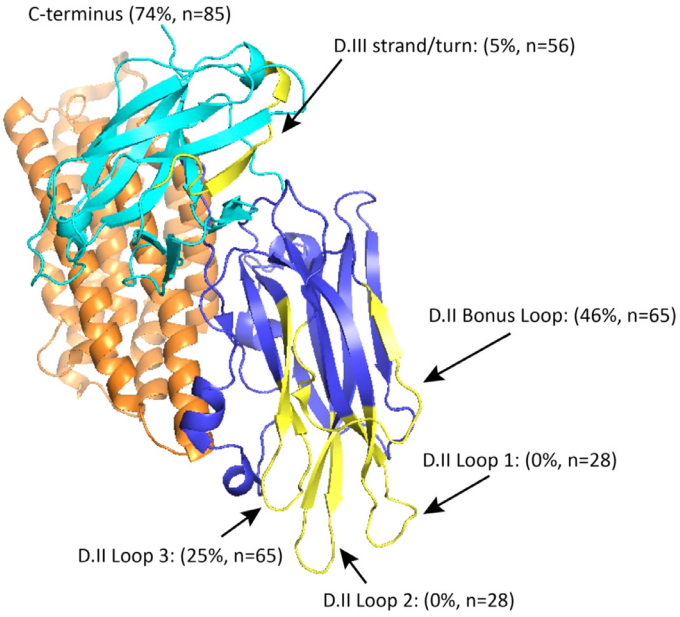

Figure 2. Sites in Cry3Bb1 used for peptide insertion. The amino acid regions used for peptide insertion in domains II (D.II) and III (D.III) are indicated. For each region, the percentage of variants that retained activity against Cry3Bb1-susceptible WCR and the number produced and tested are indicated.

2.4.3. Expression and purification of Cry3Bb1 variants

N-terminal His-tagged Cry3Bb1 variants and wild type Cry3Bb1 were expressed in *E. coli* Rosetta2 (DE3) cells using standard growth conditions for *lac* promoter induction in media with 1 mM IPTG and 100 ug/ml kanamycin and 25 μg/ml chloramphenicol and incubated at 18 °C for 48 hours. Cells were pelleted and lysed with a 3:1 mixture of B-PER and Y-PER (Thermo Fisher Scientific; Waltham, MA), 25 mM Tris-HCl pH 8, supplemented with 150 mM NaCl, 0.1 mg/ml lysozyme and EDTA free protease inhibitor cocktail (MilliporeSigma; Burlington, MA). Cleared lysate was incubated with His-Select Nickel Affinity gel (MilliporeSigma; Burlington, MA) at 4 °C for 30 min. The affinity gel was washed in buffer containing 250 mM NaCl, 30 mM Tris-HCl pH 8.0, 10 mM imidazole and eluted in a buffer of 250 mM NaCl, 30 mM Tris-HCl pH 8.0, and 200 mM imidazole. Further purification of eluted proteins was conducted using a HiTrap Q HP column (GE Healthcare) using a salt gradient from buffer A containing 50 mM sodium carbonate pH 9.0 to buffer B containing 50 mM sodium carbonate pH 9.0 and 1M NaCl, with a final elution resulting in approximately 200mM NaCl.

2.5. Cry3Bb1 variant properties and bioactivity

2.5.1. Stability of Cry3Bb1 variants

To analyze variant stability against proteolytic digestion, selected variants were incubated with bovine pancreatic trypsin (10% w/w of insecticidal protein) overnight at 37 °C. To determine stability in WCR gut juice, a total of 10 μg of native or modified Cry3Bb1 was incubated with 3.4 μl gut juice in a final volume of 10 μl for 1hr or over-night at RT. Samples were solubilized with Laemmli sample buffer and proteins analyzed by resolving in a 4-20 % SDS PAGE gradient gel stained with Coomassie Brilliant Blue. An untreated Cry3Bb1 sample was included as a positive control.

2.5.2. Relative binding of wild type and variant Cry3Bb1

To assess relative binding of modified and wild type Cry3Bb1, pull-down assays were conducted with BBMV. Modified Cry3Bb1 proteins (100 nM) were incubated with 10 μg s-WCR BBMV in binding solution (1xPBS 0.1% Tween 20 and 0.1% BSA) in a final volume of 100 μl. This solution was incubated for 1 hour with constant shaking of 70

rpm at RT, then centrifuged at 20,800 g for 20 min at 4 °C. The pellet was resuspended in 100 μl of binding buffer, and centrifugation was repeated 3 times. The resulting pellet was resuspended in 10 μl of binding buffer, boiled in Laemmli sample buffer, and proteins analyzed by western blot. Proteins were resolved in a 4-20% SDS PAGE gradient gel and transferred to a PVDF membrane (MilliporeSigma; Burlington, MA). The membrane was blocked with 1X TBS 0.2% Tween 20 and 5% BSA. Cry3Bb1 was detected using an anti-His monoclonal antibody (Thermo Fisher Scientific; Waltham, MA) at a dilution of 1:2500, a secondary goat anti-mouse HRP coupled antibody (Thermo Fisher Scientific; Waltham, MA) at a dilution 1:5000, and supersignal west femto chemiluminescent substrate (Thermo Fisher Scientific; Waltham, MA). The density of the signal obtained was analyzed using imaging software on the FluorChem M FM0591 instrument (ProteinSimple; San Jose, CA)

2.5.3. WCR bioassays

Cry3Bb1-susceptible and -resistant WCR strains (Flagel et al. 2015; Willse, Flagel, and Head 2021; Moar et al. 2017). were used to evaluate pesticidal protein efficacy in larval artificial diet bioassays using a modified protein overlay method (Yin et al. 2020). Bioassays were conducted for 6 days at 27 ºC and 70% relative humidity and included 3 replicates with 24 insects per treatment. The positive control in the assay was wild-type Cry3Bb1 with ≥ 85% mortality expected at a dose of 1mg/ml (1000ppm). To streamline the screen, the protein concentration of variants tested was not normalized yet included a dose of at least 1mg/ml (1000ppm) per variant sample in diet overlays to enable relative activity comparisons vs. the controls. Negative controls included buffer-only diet overlays and resultant material from an empty cloning vector tested in parallel with the new variants during protein expression. Statistically significant activity was determined as pesticidal proteins causing greater mortality to WCR larvae relative to the negative controls according to a one-sided Wilcoxon Rank Sum test ($p < 0.05$). As our goal was to overcome resistance in WCR rather than improve activity against susceptible WCR, experiments and analyses to directly assess performance of variants relative to wild type Cry3Bb1 (i.e. LC_{50} bioassays) were not conducted in either colony.

3. Results

3.1. Targets for phage display

Four different targets for phage display were produced in this study, including BBMV from Cry3Bb1-susceptible and Cry3Bb1-resistant insects, WCR APN and CAD. BBMV preparations (Fig. S1) were assessed by monitoring leucine-aminopeptidase activity. This activity increased 3.2 to 4.3-fold in BBMV derived from s-WCR, and 4.9-fold in BBMV from r-WCR relative to midgut homogenates, indicating suitable enrichment of this reagent to proceed with biopanning against phage display libraries. Expression of recombinant targets WCR APN and CAD enabled purification of proteins used for biopanning (Fig. S2).

3.2. Phage display and peptide identification

Three rounds of biopanning were completed for each of the four phage display targets against two commercially available libraries, Ph.D.™-C7C and Ph.D.™-12. A combination of Sanger sequencing and deep sequencing was used to characterize phage pools selected from rounds 2 and 3 of each biopanning experiment. Candidate phage display-derived binder sequences identified by Sanger sequencing and selected for Tier-1 engineering on the basis of combined selection criteria (ELISA, stability, enrichment, target) are provided in Tables S2 and S3. All peptide sequences identified by MiSeq are provided in File S2. Computational analyses were conducted on Sanger-sequenced phage peptides to generate data regarding their potential suitability for Cry3Bb1 engineering. Twelve of 15 peptides selected from Ph.D.™-C7C and 15/26 peptides from Ph.D.™-12 against BBMV were predicted to be hydrophilic in nature according to their GRAVY score (Table 1). Peptides from the second and third rounds of WCR APN biopanning included 11/15 and 13/28 peptides predicted to be stable from the Ph.D.™-C7C and Ph.D.™-12 libraries, respectively (Table 1).

3.3. Validation assays

3.3.1. Evaluation of peptide binding

ELISA was used as a screen to assess binding of a subset of peptides on isolated phage clones to selected targets. Binding to s-WCR BBMV was confirmed for 15/15 peptides selected from the Ph.D.™-C7C screen and 24/29 of those from the Ph.D.™-12 library screen (Fig. S3). Binding to r-WCR BBMV was confirmed for all selected phage clones assayed including 19 Ph.D.™-C7C-derived and 29 Ph.D.™-12-derived peptides. Binding to s-WCR BBMV was confirmed for all 30 Ph.D.™-C7C-derived peptides and 33 Ph.D.™-12-derived peptides that were selected for binding to WCR CAD (Fig. S4). A total of 7/15 peptides from the Ph.D.™-C7C screen against APN bound to recombinant WCR APN in the ELISA (Fig. S4). Of the Ph.D.™-12-derived peptides, 23/29 bound recombinant APN and 28/29 bound s-WCR BBMV (Fig. S4, Table S4).

3.3.2. Identification of peptide binding partners

Selected peptides were synthesized with biotin and Bpa modifications at the N- and C-termini, respectively for use in UV-crosslinking experiments to identify candidate binding targets from Cry3Bb1 s-WCR BBMV. Western blot analysis was used to confirm if selected peptides 21 (NFWSAAYPLGTL), 56 (CQPFTTYRC), 87 (HDGYWWHSMTMW) and 223 (CPLAYPHTC) (Table 2) along with peptide 19 (CLREESGQC; Ph.D.™-C7C, APN target) UV-crosslinked to BBMV proteins Table 2. provides the criteria used for selection of peptides 21, 56, 87 and 223. Peptide 19 was used for comparison of binding with peptide 21 (Ph.D.™-12, APN target). Unique protein bands were evident in UV crosslinked lanes (Fig. S5). Both UV and non-UV lanes were cut into four equal sized sections (Fig. S5) and used for LC-MS/MS analyses. Between 4 and 8 unique cell surface proteins were identified as binding partners for each of the peptides when tested with s-WCR BBMV (Table 3).

Several of the gut surface binding proteins, including aquaporin, ABC transporters (including multidrug resistance-associated protein 1), aminopeptidase N-like, transferrin-like isoform 1, bound to multiple peptides. The binding partners of peptide 87, which was selected for binding to r-WCR BBMV, were determined in both s-WCR and r-WCR BBMV with a total of 8 and 13 binding proteins identified, respectively (Table 3). While the multidrug resistance associated proteins, transferrin and cadherin appeared in both of these screens, five peptide 87 binding proteins identified in the UV lane for r-WCR BBMV were absent from both the UV or non-UV control lane for s-WCR BBMV (Table 3). Similarly, several s-WCR BBMV proteins with the highest SequestHT scores (including plasma membrane calcium-transporting ATPase 2 isoform X3 and aminopepidase N-like) were not enriched in UV-crosslinked samples with r-WCR BBMV.

3.3.3. Peptide-mCherry pulldown assays

A small-scale screen was conducted to understand the relative strength of binding and binding specificity of selected peptide-mCherry fusions to s-WCR BBMV. Pull-down competition assays were performed with peptides 21, 56, 87 and 223. The Ph.D.™-C7C-derived peptide-mCherry fusion proteins (peptides 56 and 223) bound specifically to s-WCR BBMV, and binding decreased in competition with an increasing amount of the same peptide labelled with biotin (Fig. S6). In contrast, the Ph.D.™-12-derived peptide-mCherry fusion proteins (peptides 21 and 87) showed relatively lower levels of binding than Ph.D.™-C7C peptides and did not show specific binding. ImageJ quantification of band intensity to estimate the relative amount of peptide-mCherry associated with s-WCR BBMV confirmed reduced binding of peptide-mCherry in the presence of peptide-biotin, with clear displacement of

Table 1
Candidate gut binding peptides screened against BBMV in ELISA. Peptides selected for binding to s- or r-WCR-derived BBMV are arranged in order of decreasing binding to s-WCR BBMV in ELISA. Gravy scores and instability indices are shown. Hydrophobic peptides and peptides predicted to be stable are indicated in italics. Proteins with a positive GRAVY score are hydrophobic, and proteins with an instability index of <40 are predicted to be stable. Tier 1 peptides selected for Cry3Bb1 modification are shown in bold. Phage names are indicated as identifiers for storage and recovery purposes.

OD ratio ELISA	Phage Name	Peptide Sequence	Gravy Score	Instability Index	OD ratio _ELISA	Phage Name	Peptide Sequence	Gravy Score	Instability Index
7.34	rr7_28	QLSKLLR	-0.19	*23.96*	14.99	rr12_59	PHDDVLWLHPS	-0.59	56.73
7.06	rr7_14	EHRRRIR	-2.89	161.46	14.88	rr12_62	VLHGHSADPAPK	-0.55	*25.55*
6.50	ss7_R316	QSHPGPF	-1.19	94.74	14.47	rr12_54	HSLRHDWKYNSV	-1.47	41.27
6.34	ss7_R234	HLEPTKQ	-1.80	69.91	14.32	rr12_80	SPHTERAHSVAT	-0.93	48.48
6.33	rr7_4	GPLFGWN	-0.03	43.83	**14.27**	**rr12_87**	**HDGYWWHSMTMW**	**-1.00**	***10.78***
6.07	rr7_41	SLGHSVV	*1.00*	*8.57*	14.26	rr12_91	HSLRHDWKYNSV	-1.47	41.27
6.06	ss7_R373	PGILSWG	*0.60*	*9.14*	14.24	rr12_79	DSMFLAHLLTPG	*0.64*	*18.14*
5.94	rr7_3	TRTYHNF	-1.59	*38.56*	9.99	ss12_5	TLSLPGFTFVPT	*0.91*	51.55
5.83	rr7_10	GPVMPHA	*0.16*	98.86	8.21	ss12_12	IDYTMPLSFSGF	*0.56*	*38.71*
5.55	rr7_25	EPSSYKH	-2.16	91.11	8.03	rr12_84	HVNYHTLTLTFV	*0.46*	*23.45*
5.47	rr7_46	WHDKSHQ	-2.71	*30.27*	7.95	ss12_34	LSDSKERIRFQ	-1.26	*26.60*
5.40	ss7_R232	FNNASSK	-1.13	*36.09*	7.72	rr12_52	LMNSAPWPLGVA	*0.71*	*22.82*
4.90	**ss7_R223**	**PLAYPHT**	**-0.40**	***15.43***	6.84	ss12_4	GPVYIEFTTWMP	*0.23*	99.38
4.73	ss7_R214	TNTLRNQ	-1.80	*9.34*	6.83	ss12_6	FILRIMCVGVFV	*2.54*	*27.91*
4.66	rr7_24	DRFRLPQ	-1.57	52.83	6.60	rr12_81	NIRWELTMAHLH	-0.31	96.73
					5.90	ss12_24	TQSYPNPTSPTL	-1.08	84.00
					5.20	ss12_17	SPHTERAHS	-1.83	61.30
					5.07	ss12_22	STPPYTHLHAGF	-0.43	*18.14*
					4.41	ss12_15	RSILVIIIILRR	*1.67*	141.67
					4.40	rr12_85	NIRWELTMAHLH	-0.31	96.73
					3.33	ss12_39	LAHSNHVLPLSQ	*0.07*	*34.19*
					3.31	rr12_86	HSLRHDWKYNSV	-1.47	41.27
					3.12	ss12_46	TWWWTTTQVLTA	*0.01*	*-28.45*
					2.84	ss12_42	TNHWDDALLTES	-0.91	*26.34*
					2.67	rr12_82	HSLRHDWKYNSV	-1.47	41.27
					2.28	ss12_43	IVDSVGCVAA	*1.85*	*-11.29*

Table 2
Criteria for selection **of four Tier 1 peptides for Cry3Bb1 modification.** Phage names indicated as identifiers for storage and recovery purposes. R: round of panning analyzed by MiSeq.

Phage Name:	APN_21	rr12_87	APN_56	ss7_R223
Peptide:	**21**	**87**	**56**	**223**
Sequence	NFWSAAYPLGTL	HDGYWWHSMTMW	CQPFTTYRC	CPLAYPHTC
Library:	Ph.D.™-12	Ph.D.™-12	Ph.D.™-C7C	Ph.D.™-C7C
ELISA score: Plate coating	>2: APN, BBMV	>14: BBMV	>3: BBMV; 1.9: APN	>5 BBMV
Instability index	Stable	Stable	Stable	Stable
MiSeq abundance note	3rd most abundant: APN R3	Abundant: r-WCR BBMV R3	Abundant: APN R3	Abundant: CAD R2 and s-/r-WCR BBMV R2-R3
MiSeq Enrichment Rounds 2-3	125X: APN	1.4X, 13 X: s-/r-WCR BBMV, respectively	2.5X: APN	4X: r-WCR BBMV
Trypsin sensitive	No	No	Potentially	No

peptide-mCherry bound to BBMV by 1000 mM of peptide biotin (Fig. S6).

3.4. Cry3Bb1 engineering

3.4.1. Tier 1 Cry3Bb1 variants

Four peptides were chosen as top candidates for the first round (Tier 1) of protein engineering of Cry3Bb1 based on their combined data from ELISA, stability and enrichment in Miseq analyses of phage pools and target selection (Table 2). These included two peptides each from the Ph.D.™-C7C and Ph.D.™-12 libraries that were inserted into six different regions on the Cry3Bb1 scaffold (Fig. 2) using a tiling approach (File S1). A total of 144 Cry3Bb1 variants were designed featuring Tier 1 peptide insertions, and 140 variants (97%) were successfully cloned and produced (Fig. S7; File S1).

3.4.2. Tier 2 Cry3Bb1 variants

Activity scores relative to position effects of Tier 1 peptide insertions and bioassay results (see 3.5.2) were used to guide Tier 2 peptide insertions in the Cry3Bb1 scaffold. A second round of 183 variants were designed based on the outcome of the first round, where sites were prioritized to insert a wider variety of peptide binder sequences for screening. The C-terminus (Ph.D.™-C7C and Ph.D.™-12 peptides) and insertion into positions 394-402 (Ph.D.™-C7C -specific), 494-502 (Ph.D.™-C7C -specific), and 559-570 (Ph.D.™-12 -specific) were selected for further engineering (note that these position locations include a 10 amino acid flexible linker-His tag addition at the N-terminus relative to the wild type Cry3Bb1 sequence). A total of 73 peptides (37 Ph.D.™-C7C; 36 Ph.D.™-12) were selected from biopanning experiments based on combined criteria from ELISA and/or MiSeq analyses (File S1) and used to construct 183 Cry3Bb1 variant designs in Tier 2. Of these, 144 were successfully cloned (79%), produced, and tested in the Cry3Bb1 susceptible WCR diet bioassay; 39 variants (21%) failed during the cloning process and were not remediated.

3.5. Characterization of Cry3Bb1 variants

3.5.1. Stability of Cry3Bb1 variants

Trypsin and gut juice digests were conducted for 5 tier 1 variants (#15, 16, 93, 110, and 138) to provide a snapshot of Cry3Bb1 stability

Table 3

Gut membrane binding partners of selected peptides. Proteins that were unique to the UV-exposed lane, or ≥ 2 fold peptide spectrum match (PSM) in UV compared to non-UV samples (indicated by *) are shown. The presence of each protein in fractions F1 to F4 as indicated in Fig. S5 is also shown. Assays were conducted with BBMV from susceptible WCR (s-WCR) unless otherwise indicated. For binding partners of peptide 87, the five proteins in italics were present in BBMV derived from resistant WCR (r-WCR) but not in those from s-WCR.

Protein [*Diabrotica virgifera virgifera*]	Unique Peptides	Peptides	PSMs	MW (Kda)	SequestHT score	Present in Fractions	Coverage %
Peptide 223 (Ph.D.™-C7C, s- WCR BBMV target)							
Plasma membrane calcium-transporting ATPase 2 isoform	13	13	15	134.6	39.52	F1	14
Multidrug resistance-associated protein 1 isoform X1	4	4	4	106	11.6	F1	6
CD63 antigen-like isoform X2	2	2	2	25.5	8.42	F4	13
Aquaporin AQPAe.a-like	2	2	3	28.6	8.33	F4	9
Transferrin-like isoform X1	2	2	2	79.9	6.22	F3	4
Peptide 56 (Ph.D.™-C7C, APN target)							
Probable multidrug resistance-associated protein lethal (2)03659	4	5	7	149.1	13.97	F1	5
ATP-binding cassette sub-family D member 3	3	3	3	73.8	6.15	F1, F2	4
ABC transporter G family member 23	2	2	3	85.4	6.75	F2	4
Neprilysin-2 isoform X1	2	2	2	88.8	6.05	F1	3
Aquaporin AQPAe.a-like	2	2	3	28.6	8.22	F4	9
Aminopeptidase N-like	10	10	11	105.6	31.47	F1	12
Aminopeptidase N-like*	4	4	5	105.6	15.5	F1	5
Peptide 87 (Ph.D.™-12, r-WCR BBMV target); **s-WCR BBMV**							
plasma membrane calcium-transporting ATPase 2 isoform X3	11	16	17	134.6	46.17	F1	18
aminopeptidase N-like	12	12	14	105.6	40.05	F1	14
transferrin-like isoform X1	5	5	5	79.9	12.26	F1, F2, F3	8
CD63 antigen-like isoform X2	4	4	4	25.5	11.95	F4	21
neprilysin-2 isoform X1	4	4	4	88.8	11.51	F1	7
multidrug resistance-associated protein 1 isoform X1	3	4	4	106	10.68	F1	5
probable multidrug resistance-associated protein lethal(2)03659	2	2	2	155.5	5.99	F1	2
cadherin-23-like	3	3	3	191.2	5.69	F1	2
Peptide 87 (Ph.D.™-12, r-WCR BBMV target); **r-WCR BBMV**							
cadherin-23-like	6	6	6	191.2	20.29	F1	5
probable multidrug resistance-associated protein lethal(2)03659 isoform X1	3	5	6	153	15.87	F1	4
multidrug resistance-associated protein 1-like	4	4	5	45.7	14.84	F1	9
monocarboxylate transporter 3 isoform X1	4	4	4	86.9	11.88	F1, F2	7
ATP-binding cassette sub-family D member 3	6	6	6	73.8	10.92	F2	9
plexin domain-containing protein 2	2	2	2	62.1	8.89	F2	9
ATP-binding cassette sub-family G member 4-like	3	3	3	76.5	8.63	F1, F2, F3	5
protein THEM6-like isoform X1	2	2	3	25.3	7.98	F1, F2, F4	12
copper-transporting ATPase 1 isoform X1	4	4	4	139.1	7.93	F1	4
NPC intracellular cholesterol transporter 1 homolog 1b-like	3	3	3	92.6	7.58	F1	4
glutamate receptor ionotropic, kainate 4-like	2	2	2	57.6	6.78	F1, F2	6
nose resistant to fluoxetine protein 6-like	2	2	2	76.5	6.19	F1	4
transferrin-like isoform X1	11	11	12	79.9	32.91	F2, F3	17
transferrin-like isoform X1*	5	5	5	79.9	15.17	F2, F3	11
Peptide 21 (Ph.D.™-12, APN target)							
aminopeptidase N-like	3	3	5	105.6	8.99	F1	3
alpha-amylase	2	7	9	53.2	25.07	F2	19
receptor-like protein 9a	3	3	3	113.4	7.49	F2	4
aquaporin AQPAe.a-like	2	2	4	28.6	10.21	F4	9
Peptide 19 (Ph.D.™-C7C, APN target)							
probable multidrug resistance-associated protein lethal(2)03659	4	5	7	149.1	13.97	F1	5
ATP-binding cassette sub-family D member 3	3	3	3	73.8	6.15	F1, F2	4
ABC transporter G family member 23	2	2	3	85.4	6.75	F2	4
neprilysin-2 isoform X1	2	2	2	88.8	6.05	F1	3
aquaporin AQPAe.a-like	2	2	3	28.6	8.22	F4	9
aminopeptidase N-like	10	10	11	105.6	31.47	F1	12
aminopeptidase N-like*	4	4	5	105.6	15.5	F1	5

under conditions simulating the gut environment in WCR larvae (Fig. S8). The stability of 3 (16, 110, 138) out of five variants was comparable to that of wild type Cry3Bb1 in overnight assays, whereas 2 variants (15, 93) were completely digested during the treatment (both digested variants contained the potentially trypsin prone peptide CQPFTTYRC). Pull down assays were conducted for Cry3Bb1 variants against s-WCR BBMV. Relative to the wild type CryBb1 protein, variants 15 and 16 (File S1) showed enhanced binding to BBMV in both replicates while variant 138 had increased binding in the second replicate only (Fig. 3).

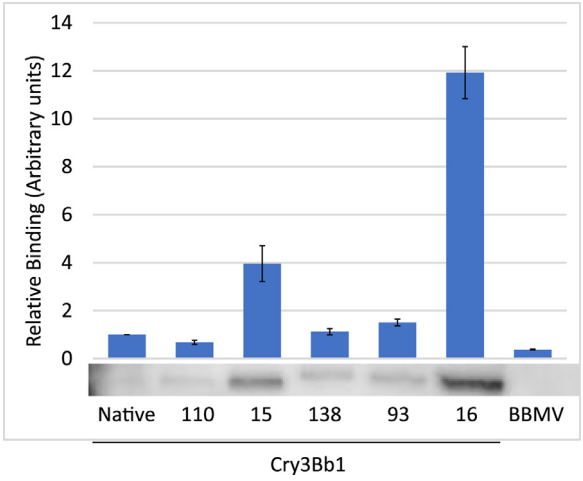

Figure 3. Relative binding of native and variant Cry3Bb1 to s-WCR BBMV. Relative intensities of Cry3Bb1 bands in this representative western blot-pull down assay was quantified with FlourChem M FM0591 imaging software. Binding to BBMV was increased for a subset of variants relative to native Cry3Bb1. Variant 138 also showed increased binding in a single replicate (not shown).

3.5.2. Tier 1 variant bioassays

The 140 Tier 1 variants were tested in an artificial diet bioassay screen to assess the impact of peptide modification on Cry3Bb1 activity in WCR larvae (File S1). The screen was designed to initially assess insecticidal activity in the Cry3Bb1 susceptible colony and then follow up with top hits then assayed against the resistant colony. Of these Tier 1 variants, 22 (16% of those tested) caused significant mortality comprised of 12 and 10 insertions of Ph.D.™-C7C and Ph.D.™-12 peptides, respectively. All C-terminal insertions were at least moderately active (50-75% mortality), and 6 of these variants were highly active (> 75% mortality). Seven variants with low (statistically significant, but with less than 50% mortality) and moderate (50-75% mortality) activity scores were observed in insertions to the DII "bonus-loop", DII loop 3 and DIII strand/turn. No active variants were observed for insertions in DII loops 1 or 2. In DII loop 3, active variants were produced with either Ph.D.™-C7C or Ph.D.™-12 peptide insertions. Activity in the s-WCR colony correlated with results from the selected variants screened in the above digestion assays; variants 16, 110 and 138 that were relatively stable were also active, while the unstable variants 15 and 93 did not cause statistically significant mortality in the bioassay. Variant 15 nearly missed the cutoff for significance in the bioassay, and 3 other tier 1 variants containing this peptide were active (2 with DII loop 3 insertions and one variant with a C-terminal addition), which indicated that stability and activity may be position specific regarding peptide placement in the scaffold. Sixteen of the most active Tier 1 variants were tested in the Cry3Bb1-resistant WCR colony diet bioassay, but none caused statistically significant mortality in the screen, and thus were deemed ineffective in overcoming resistance.

3.5.3. Tier 2 variant bioassays

The 144 Tier 2 variants that were successfully produced were tested in the Cry3Bb1 susceptible WCR diet bioassay. A total of 90 variants (63% of those tested) caused statistically significant mortality in the Cry3Bb1 susceptible WCR diet bioassay screen. Consistent with results from Tier-1 variant testing, the pool of C-terminal peptide insertions from both libraries contained several variants with high activity in the susceptible WCR colony (File S1). The DII bonus loop insertions of Ph.D.™-C7C peptides had the highest proportion of active variants designed and tested, and also included multiple highly active variants (> 75% mortality), whereas the DIII Strand/Turn insertions of Ph.D.™-12 peptides had the lowest proportion of active variants. No statistically significant mortality was observed for the 90 active Tier-2 variants in the Cry3Bb1-resistant WCR colony screen.

4. Discussion

Development of resistance in WCR against commercially-deployed Bt pesticidal proteins expressed in transgenic corn is an ongoing challenge for the agricultural industry (Gassmann 2021), and new approaches are needed for continued use of transgenic plant biotechnology for crop protection (Yin et al. 2020; Bowen et al. 2020). We employed peptide-mediated engineering of Bt-derived pesticidal proteins, which has proven effective in generating novel insecticidal proteins (Chougule et al. 2013; Mishra et al. 2021; Shao et al. 2016; Vilchez 2020) to test a receptor-retargeting approach to restore insecticidal activity against Cry3Bb1-resistant WCR. This approach was designed to extend the longevity and efficacy of Cry3Bb1, which has a history of safe use and broad deployment for managing WCR damage in corn.

4.1. Identification of sites suitable for peptide modification of Cry3Bb1

This screen included 77 peptides used to engineer and successfully produce 284 new Cry3Bb1 variants. While none of these variants displayed activity against the Cry3Bb1-resistant WCR colony, several groups of variants retained insecticidal activity against Cry3Bb1-susceptible WCR. This demonstrated that Cry3Bb1 can be engineered using 7-12-mer amino acid peptide insertions from phage libraries that result in new protein variants with high insecticidal activity and potential for delivering new receptor-binding interactions depending on the peptide content and insertion site.

Sites in the Cry3Bb1 scaffold selected for engineering peptide insertions or replacements were guided by knowledge of receptor binding interfaces of three domain Cry proteins and thus deemed as having potential for receptor retargeting. For example, DII loops mediate receptor interactions required for insecticidal activity and the DIII strand in Cry1A mediates APN binding (Pacheco et al. 2009; Zhang, Hua, and Adang 2017). Results from the Tier-1 peptide modified experiments (four peptides; six insertion regions) provided a framework for a more sequence-diverse but site-targeted engineering effort in Tier-2 (73 peptides, four insertion regions), based on suitability of positions for engineering relative to insecticidal activity observed. Indeed, more active variants were generated in Tier-2 relative to Tier-1 engineering, demonstrating progress in our understanding of Cry3Bb1 scaffold amenability for peptide insertions. The top performing variants that had significant activity against the Cry3Bb1-susceptible colony had peptides attached to the C-terminus or inserted into one of three different loops (D394-L403, C491-I501, S557-N568). Of these, the C terminus and DII bonus loop were the best positions for peptide addition regarding production of biologically active variants. It is possible that peptide insertions in active variants did not impact binding to the native receptor nor influence properties critical for a response, while being unable to initiate new receptor interactions needed for effective retargeting. In contrast, insertions into DII loops 1 and 2 resulted in significant losses of insecticidal activity. The latter may reflect changes in critical binding regions needed to interact with the native Cry3Bb1 receptor or influencing features needed for downstream events leading to insecticidal activity.

Learning cycles from such gain/loss of activity studies based on position effect of peptide replacements may prove key for future engineering strategies. For example, peptides identified from library screens against specific targets described herein, or additional targets, could be engineered into the known amenable engineering positions and theoretically improve both retargeting against resistant WCR populations while maintaining Cry3Bb1 activity against susceptible WCR populations through the native receptor(s). Increased binding to BBMV demonstrated for variants #15 and 16 represented a promising finding, although as noted previously (Chougule et al. 2013), enhanced binding does not guarantee

increased insecticidal properties, as was shown here where the stability of these variants was compromised.

In addition to position effect, binder sequence composition is another key component required for successful retargeting. Diverse peptide sequences were engineered into the Cry3Bb1 scaffold from both libraries tested; however, none were able to bring new activity against Cry3Bb1-resistant WCR. However, evidence from the ELISA and BBMV-binding assays supported the phage display selection process for revealing binding entities from each library to different targets. From a structural standpoint, the Ph.D.™-C7C and Ph.D.™-12 libraries differ not only in peptide length but also with the former being more rigid due to the Cys-Cys linkage relative to the more flexible 12-mer peptides. Insertion positions for the peptides included flexible loop segments of Cry3Bb1 to improve the probability that binding surfaces could be maintained relative to the context observed in phage particles. Structural comparisons of peptide-receptor interactions in the context of the phage and the protein scaffold and how this impacts binding and affinity would require empirical work beyond the scope of the current screen. One potential solution to minimize issues associated with changing flanking regions of selected peptide binders (e.g. from phage to pesticidal protein) is to create diverse libraries in regions of interest (e.g. domain II loops) within the entire protein scaffold displayed on the phage surface (Kasman et al. 1998).

4.2. Stability of Cry3Bb1 variants

At the outset of this work, the possibility that amino acid replacements of such length could lead to entirely unstable, inactive proteins was not excluded. However, this was not the case, as all variants appeared to maintain proper expression profiles but with varying levels of relative stability, and with activity ranging from 0-100% mortality in Cry3Bb-suscpetible WCR diet bioassays. Any constructs for which peptide insertion into the Cry3Bb1 scaffold resulted in alterations in structure, stability in the WCR gut, or binding capability were eliminated from further analysis as activity against Cry3Bb1-susceptible WCR was lost. Indeed, three of five variants had comparable stability to Cry3Bb1 in overnight protease digestions, while two were completely digested, suggesting that variant stability is an attribute that should be monitored closely to refine future engineering and screening processes.

4.3. Peptide binding partners on the surface of the WCR gut epithelium

Candidate gut binding partners for the four Tier-1 peptides resulting from BBMV, or APN screens, along with peptide 19 selected for binding to APN were identified. For peptides selected for binding to recombinant APN, binding to WCR aminopeptidase N-like was confirmed. However, while the greatest coverage and SequestHT score for the Ph.D.™-C7C-derived peptide 19 was aminopeptidase N-like, the highest scores for the Ph.D.™-12-derived peptide 21 was alpha-amylase, even though both peptides were selected for binding to recombinant WCR APN. This result may reflect increased binding specificity of the shorter, constrained, Ph.D.™-C7C-derived peptides. Interestingly, the peptide-mCherry competition assays showed that peptides 223 and 56 (both derived from Ph.D.™-C7C) bind specifically (Fig. S6), while peptides 21 and 87 (derived from Ph.D.™-12) did not. Given the relative lengths of these peptides (7 versus 12 amino acids), the lack of structure of the longer peptide may provide for additional binding partners relative to the cysteine-constrained loop of Ph.D.™-C7C-derived peptides. However, further analysis of binding strength and consideration of relative protein abundance on the surface of midgut microvilli would be needed to elucidate the primary gut binding partner in each case.

The identification of multiple binding partners for each peptide highlights the potential for even a short 7 amino acid peptide loop to bind to multiple proteins, with a few amino acids sufficient for protein-protein interaction. In addition, weak non-specific interactions with BBMV proteins may be detected by UV-crosslinking. The peptide binding partners included proteins expected to be abundant on the surface of the gut epithelium and previously implicated in Bt pesticidal protein mode of action, such as aminopeptidase N-like and cadherin (Zhang, Hua, and Adang 2017; Guo et al. 2020). Several of the binding proteins such as aquaporin, a channel protein that allows water to move rapidly across cell membranes, are not known as receptors for bacterial pesticidal proteins, but are implicated in some instances in pesticidal protein mode of action (Endo et al. 2017).

For peptide 87, which was selected for binding to r-WCR BBMV, five of the binding partners in r-WCR BBMV were unique, and not detected in s-WCR BBMV (Table 3). In addition, proteins bound frequently by peptide 87 in s-WCR BBMV were not enriched on UV crosslinking with r-WCR BBMV. It is unclear whether these results have any significance in relation to the mechanism of Cry3Bb1 resistance.

4.4. Lack of insecticidal activity against Cry3Bb1 resistant WCR

Pesticidal protein retargeting to alternative, abundant gut surface receptor proteins has been demonstrated in other insects (Chougule et al. 2013), but was not successful in overcoming Cry3Bb1 resistance in WCR with the engineered variants tested herein. Considerations for this result include 1) the nature and orientation of binder peptide-receptor interactions *in vivo*, 2) potential for non-productive binding (in the case where binding partners are not functional Bt receptors, insufficiently abundant to drive a response in midgut cells, or binding is not strong enough to trigger required conformational changes), 3) irreversible binding to a non- receptor, or 4) events subsequent to binding required for pore formation. While aminopeptidase activity indicative of appropriate folding was demonstrated for the recombinant APN produced in Sf21 cells (derived from a lepidopteran insect), there may be differences in post-translational modifications or inaccessible surfaces when compared to WCR APN. Future studies may benefit from screening against a wider range of recombinant gut surface proteins selected based on comprehensive proteomic examination of WCR midgut cells, and potentially including ABC transporter proteins (see 4.5). However, given the prior demonstration of the utility of gut binding peptides selected to target alternative gut surface proteins using comparable approaches (Mishra et al. 2021) and the testing of 93 peptide-modified Cry3Bb1 variants, it is possible that alteration of Cry3Bb1 binding is not the basis for resistance in WCR (see 4.5).

4.5. Role of ABC transporters in Cry3 resistance

The binding partners of peptide 87 include several ABC transporter proteins. Some of the ABC transporters function as putative receptors for Bt pesticidal proteins in insects (Heckel 2012; Tay et al. 2015; Wu et al. 2019; Atsumi et al. 2012), and alterations in ABCB1 is involved in Cry3A resistance in Coleoptera (Niu et al. 2020; Pauchet et al. 2016). Mechanisms of ABCB1-mediated resistance include down-regulation of the transcript (Guo et al. 2015), mutation of the coding sequence, frameshifting and production of alternative transcripts (Niu et al. 2020; Pauchet et al. 2016; Heckel 2021). Based on mapping of Cry3Bb1 resistance genes (Flagel et al. 2015; Willse, Flagel, and Head 2021), it seems likely that ABCB2 may function similarly in WCR Cry3Bb1 resistance.

If WCR ABCB2 or a related protein functions solely as a receptor for Cry3Bb1 and if expression was altered in r-WCR such that Cry3Bb1 binding was reduced or blocked, we would expect to restore activity by use of peptide 87 or other peptides that bind other gut surface proteins such as APN or cadherin. This expectation is based on the successful application of gut binding peptides to enhance the activity of pesticidal proteins (including Cry1Ab) via binding to novel gut surface proteins (Chougule et al. 2013; Shao et al. 2016). If, however, WCR ABCB2 is required as an essential, dynamic component in Cry3Bb1-mediated pore formation downstream of binding as previously postulated (Heckel 2021), loss of that functionality would not be restored by binding to alternative gut surface proteins. ABC transporters could

therefore function 1) as three-domain Cry protein receptors, 2) in pore formation, or 3) both as receptor and in pore formation.

The lack of activity of any of the 93 Cry3Bb1 variants tested against r-WCR suggests that either ABCB2 or another component involved downstream of binding is required for Cry3Bb1 activity against r-WCR, and if ABCB2 functions as a receptor that selected peptides did not bind to ABCB2. It follows therefore that 1) selection of peptides against recombinant ABCB2 might overcome this barrier *if* the protein is expressed even at a low level and if ABCB2 functions as a receptor, 2) downregulation of ABCB2 in Cry3Bb1 resistant WCR is worthy of investigation given that the coding sequence is the same as that in susceptible WCR, and 3) that ABCB2 is likely to be required for Cry3Bb1 insertion as previously proposed (Heckel 2021; Heckel 2012). The evolution of Cry1A proteins to target ABCC transporters, Cry2A proteins to target ABCA transporters, and Cry3 to target ABCB transporters indicates a central function for different ABC transporter proteins for these three-domain proteins (Heckel 2020).

It is notable that no ABC transporters in the B family were detected as peptide binding partners in BBMV derived from Cry3Bb1-resistant or –susceptible WCR (Table 3). Members of the C family were detected (multidrug resistance-associated protein 1-like and 4-like, probable multidrug resistance-associated protein lethal(2)03659) along with ABC transporters in the D family (ATP binding cassette subfamily D member 3) and G family (ABC transporter G family member 23, ATP binding cassette subfamily G member 4-like). The identification of these six distinct ABC transporters as peptide binding partners likely reflects their abundance on the surface of the WCR gut epithelium.

5. Conclusion

As microbe-derived pesticidal proteins deployed *in planta* for suppression of pest insect populations are compromised due to emergent resistance in field populations (Gassmann 2021), identification of novel modes of action and commercially-viable pesticidal proteins is becoming increasingly challenging. Sourcing efforts have expanded outside of Bt to include pesticidal proteins derived from multiple microbial species and plants (BPPRC.org; (Crickmore et al. 2020). Protein engineering provides an expanded approach to only sourcing and mining of naturally occurring pesticidal proteins, and has the potential to improve a protein scaffold's inherent stability, binding characteristics and potency, modify the activity spectrum, or create pesticidal properties *de novo* (Mishra et al. 2021). Success toward these aims relies on increased insight into rational protein design, pesticidal protein-receptor interactions, stability and processing within the insect gut lumen, and pore forming capabilities. This study has increased our knowledge regarding each of these aspects for the Cry3Bb1 scaffold. Further, the WCR gut-binding peptides identified here may prove useful for the engineering of different pesticidal protein scaffolds in efforts to improve activity or expand target spectrum to include WCR. Taken together, these data provided insight and resources for future engineering efforts and toward elucidation of the underlying mechanism of activity and resistance to Cry3Bb1 in WCR.

Availability of data

Complete amino acid sequences for the two receptor proteins (WCR CAD and WCR APN) expressed for this study are provided in Supplementary Table 1. Full details of peptide modified Cry3Bb1 constructs including bioassay data are provided in Supplementary File 1. Details of peptides identified during rounds 2 and 3 of each phage display screen including peptide sequence and MiSeq read count are provided in Supplementary File 2.

Dedication

The authors dedicate this work to Dr. Suyog Kuwar, who passed away during preparation of this manuscript.

Declaration of Competing Interest

Bryony C. Bonning reports financial support was provided by Bayer Corp. Jason Milligan reports a relationship with Bayer Corp that includes: employment. Timothy Rydel reports a relationship with Bayer Corp that includes: employment. Zijin Du reports a relationship with Bayer Corp that includes: employment. Zhidong Xie reports a relationship with Bayer Corp that includes: employment. Sergey Ivashuta reports a relationship with Bayer Corp that includes: employment. Jean-Louis Kouadio reports a relationship with Bayer Corp that includes: employment. Jason M. Meyer reports a relationship with Bayer Corp that includes: employment.

CRediT authorship contribution statement

Suyog S. Kuwar: Methodology, Validation, Investigation, Writing – original draft, Visualization. **Ruchir Mishra:** Methodology, Validation, Investigation. **Rahul Banerjee:** Methodology, Validation, Investigation. **Jason Milligan:** Methodology, Validation, Investigation. **Timothy Rydel:** Methodology, Validation, Investigation, Visualization. **Zijin Du:** Methodology, Validation, Investigation. **Zhidong Xie:** Methodology, Validation, Investigation. **Sergey Ivashuta:** Conceptualization. **Jean-Louis Kouadio:** Conceptualization, Methodology, Validation, Investigation. **Jason M. Meyer:** Conceptualization, Methodology, Validation, Investigation, Writing – original draft, Writing – review & editing, Data curation. **Bryony C. Bonning:** Conceptualization, Writing – original draft, Writing – review & editing, Visualization, Project administration, Funding acquisition.

Acknowledgements

The authors thank Jeffrey Nageotte, Kirsten Skogerson, and Anna Bickel for research coordination and Patricia Mamanella and Budhaditya Mazumdar for assistance with protein production for diet bioassay screening. Work conducted at Iowa State University and University of Florida was funded by a grant from Bayer Crop Science, formerly Monsanto Company.

Supplementary materials

Supplementary material associated with this article can be found, in the online version, at doi:10.1016/j.cris.2022.100033.

References

Atsumi, Shogo, Miyamoto, Kazuhisa, Yamamoto, Kimiko, Narukawa, Junko, Kawai, Sawako, Sezutsu, Hideki, Kobayashi, Isao, Uchino, Keiro, Tamura, Toshiki, Mita, Kazuei, 2012. Single amino acid mutation in an ATP-binding cassette transporter gene causes resistance to Bt toxin Cry1Ab in the silkworm, *Bombyx mori*. Proc. Natl. Acad. Sci. USA 109 E1591-E98.

Badran, A.H., Guzov, V.M., Huai, Q., Kemp, M.M., Vishwanath, P., Kain, W., Nance, A.M., Evdokimov, A., Moshiri, F., Turner, K.H., Wang, P., Malvar, T., Liu, D.R., 2016. Continuous evolution of *Bacillus thuringiensis* toxins overcomes insect resistance. Nature 533, 58–63.

Ball, Harold J, Weekman, Gerald T, 1963. Differential resistance of corn rootworms to insecticides in Nebraska and adjoining states. J. Econ. Entomol. 56, 553–555.

Baum, James A, Bogaert, Thierry, Clinton, William, Heck, Gregory R, Feldmann, Pascale, Ilagan, Oliver, Johnson, Scott, Plaetinck, Geert, Munyikwa, Tichafa, Pleau, Michael, 2007. Control of coleopteran insect pests through RNA interference. Nature Biotechnol 25, 1322–1326.

Becker, J.M., Naider, F., 2015. Cross-linking strategies to study peptide ligand-receptor interactions. Methods Enzymol 556, 527–547.

Bowen, D., Yin, Y., Flasinski, S., Chay, C., Bean, G., Milligan, J., Moar, W., Pan, A., Werner, B., Buckman, K., Howe, A., Ciche, T., Turner, K., Pleau, M., Zhang, J., Kouadio, J.L., Hibbard, B.E., Price, P., Roberts, J., 2020. Cry75Aa (Mpp75Aa) Insecticidal proteins for controlling the western corn rootworm, *Diabrotica virgifera virgifera*,

(Coleoptera: Chrysomelidae), isolated from the insect pathogenic bacteria *Brevibacillus laterosporus*. Appl. Environ. Microbiol. 87. doi:10.1128/AEM.02507-20, e02507-20.

Bradford, M.M., 1976. A rapid and sensitive method for the quantitation of microgram quantities of protein utilizing the principle of protein-dye binding. Anal. Biochem. 72, 248–254.

Broehan, G., Kroeger, T., Lorenzen, M., Merzendorfer, H., 2013. Functional analysis of the ATP-binding cassette (ABC) transporter gene family of *Tribolium castaneum*. BMC Genomics 14, 6.

Chougule, N.P., Li, H., Liu, S., Linz, L.B., Narva, K.E., Meade, T., Bonning, B.C., 2013. Retargeting of the *Bacillus thuringiensis* toxin Cyt2Aa against hemipteran insect pests. Proc. Natl. Acad. Sci. USA. 110 (21), 8465–8470. doi:10.1073/pnas.1222144110.

Contreras, E., Schoppmeier, M., Real, M.D., Rausell, C., 2013. Sodium solute symporter and cadherin proteins act as *Bacillus thuringiensis* Cry3Ba toxin functional receptors in *Tribolium castaneum*. J. Biol. Chem. 288, 18013–18021.

Crickmore, N., Berry, C., Panneerselvam, S., Mishra, R., Connor, T.R., Bonning, B.C., 2021. A structure-based nomenclature for *Bacillus thuringiensis* and other bacteria-derived pesticidal proteins. J. Invertebr. Pathol. 186, 107438. doi:10.1016/j.jip.2020.107438.

Endo, H., Azuma, M., Adegawa, S., Kikuta, S., Sato, R., 2017. Water influx via aquaporin directly determines necrotic cell death induced by the *Bacillus thuringiensis* Cry toxin. FEBS Lett 591, 56–64.

Fabrick, J., Oppert, C., Lorenzen, M.D., Morris, K., Oppert, B., Jurat-Fuentes, J.L., 2009. A novel *Tenebrio molitor* cadherin is a functional receptor for *Bacillus thuringiensis* Cry3Aa toxin. J. Biol. Chem. 284, 18401–18410.

Flagel, Lex E, Swarup, Shilpa, Chen, Mao, Bauer, Christopher, Wanjugi, Humphrey, Carroll, Matthew, Hill, Patrick, Tuscan, Meghan, Bansal, Raman, Flannagan, Ronald, 2015. Genetic markers for western corn rootworm resistance to Bt toxin. G3: Genes, Genomes, Genetics 5, 399–405.

Gassmann, A.J., 2021. Resistance to Bt maize by western corn rootworm: effects of pest biology, the pest-crop interaction and the agricultural landscape on resistance. Insects 12 (2), 136. doi:10.3390/insects12020136.

Gassmann, A.J., Shrestha, R.B., Kropf, A.L., St Clair, C.R., Brenizer, B.D., 2020. Field--evolved resistance by western corn rootworm to Cry34/35Ab1 and other *Bacillus thuringiensis* traits in transgenic maize. Pest Manag. Sci. 76, 268–276.

Gassmann, Aaron J, Petzold-Maxwell, Jennifer L, Clifton, Eric H, Dunbar, Mike W, Hoffmann, Amanda M, Ingber, David A, Keweshan, Ryan S, 2014. Field-evolved resistance by western corn rootworm to multiple *Bacillus thuringiensis* toxins in transgenic maize. Proc. Natl. Acad. Sci. USA. 111, 5141–5146.

Gassmann, Aaron J, Petzold-Maxwell, Jennifer L, Keweshan, Ryan S, Dunbar, Mike W, 2011. Field-evolved resistance to Bt maize by western corn rootworm. PLoS One 6, e22629.

Gray, ME., 2012. Continuing evolution confirmed of field resistance to Cry3Bb1 in some Illinois fields by western corn rootworm. The Bulletin 20 Article 2.

Gray, Michael E., Sappington, Thomas W., Miller, Nicholas J., Moeser, Joachim, Bohn, Martin O., 2008. Adaptation and invasiveness of western corn rootworm: intensifying research on a worsening pest. Ann. Rev. Entomol. 54, 303–321.

Gubbens, J., Ruijter, E., de Fays, L.E., Damen, J.M., de Kruijff, B., Slijper, M., Rijkers, D.T., Liskamp, R.M., de Kroon, A.I., 2009. Photocrosslinking and click chemistry enable the specific detection of proteins interacting with phospholipids at the membrane interface. Chem. Biol. 16, 3–14.

Guo, Y., Carballar-Lejarazu, R., Sheng, L., Fang, Y., Wang, S., Liang, G., Hu, X., Wang, R., Zhang, F., Wu, S., 2020. Identification and characterization of aminopeptidase-N as a binding protein for Cry3Aa in the midgut of *Monochamus alternatus* (Coleoptera: Cerambycidae). J. Econ. Entomol. 113, 2259–2268.

Guo, ZhaoJiang, Kang, Shi, Chen, DeFeng, Wu, QingJun, Wang, ShaoLi, Xie, Wen, Zhu, Xun, Baxter, S.W., Zhou, XuGuo, Jurat-Fuentes, J.L., Zhang, YouJun, Guo, Z.J., Kang, S., Chen, D.F., Wu, Q.J., Wang, S.L., Xie, W., Zhu, X., Zhou, X.G., Zhang, Y.J., 2015. MAPK signaling pathway alters expression of midgut ALP and ABCC genes and causes resistance to *Bacillus thuringiensis* Cry1Ac toxin in diamondback moth. Plos Genetics 11, 1005124.

He, B., Chen, H., Li, N., Huang, J., 2019. SAROTUP: a suite of tools for finding potential target-unrelated peptides from phage display data. Int. J. Biol. Sci. 15, 1452–1459.

Heckel, D.G., 2020. How do toxins from *Bacillus thuringiensis* kill insects? An evolutionary perspective. Arch. Insect Biochem. Physiol. 104, e21673.

Heckel, D.G., 2021. The essential and enigmatic role of ABC transporters in Bt resistance of noctuids and other insect pests of agriculture. Insects 12 (5), 389. doi:10.3390/insects12050389.

Heckel, David G., 2012. Learning the ABCs of Bt: ABC transporters and insect resistance to *Bacillus thuringiensis* provide clues to a crucial step in toxin mode of action. Pesticide Biochemistry and Physiology 104, 103–110. doi:10.1016/j.pestbp.2012.05.007.

Hua, G., Park, Y., Adang, M.J., 2014. Cadherin AdCad1 in *Alphitobius diaperinus* larvae is a receptor of Cry3Bb toxin from *Bacillus thuringiensis*. Insect Biochem. Mol. Biol. 45, 11–17.

Huang, J., Ru, B., Zhu, P., Nie, F., Yang, J., Wang, X., Dai, P., Lin, H., Guo, F.B., Rao, N., 2012. MimoDB 2.0: a mimotope database and beyond. Nucleic Acids Res 40, D271–D277.

Kall, L., Krogh, A., Sonnhammer, E.L., 2007. Advantages of combined transmembrane topology and signal peptide prediction–the Phobius web server. Nucleic Acids Res 35, W429–W432.

Kasman, L.M., Lukowiak, A.A., Garczynski, S.F., McNall, R.J., Youngman, P., Adang, M.J., 1998. Phage display of a biologically active *Bacillus thuringiensis* toxin. Appl. Environ. Microbiol. 64, 2995–3003.

Kelker, M.S., Berry, C., Evans, S.L., Pai, R., McCaskill, D.G., Wang, N.X., Russell, J.C., Baker, M.D., Yang, C., Pflugrath, J.W., Wade, M., Wess, T.J., Narva, K.E., 2014. Structural and biophysical characterization of *Bacillus thuringiensis* insecticidal proteins Cry34Ab1 and Cry35Ab1. PLoS ONE 9, e112555.

Krysan, James L, and Thomas A Miller (Editors). 1986. Methods for the study of pest Diabrotica. Springer Series in Experimental Entomology, Springer, New York. 272 pp.

Kyte, J., Doolittle, R.F., 1982. A simple method for displaying the hydropathic character of a protein. Journal of Molecular Biology 157, 105–132.

Liu, S., Sivakumar, S., Sparks, W.O., Miller, W.A., Bonning, B.C., 2010. A peptide that binds the pea aphid gut impedes entry of Pea enation mosaic virus into the aphid hemocoel. Virology 401, 107–116.

Lombaert, Eric, Ciosi, Marc, Miller, Nicholas J, Sappington, Thomas W, Blin, Aurélie, Guillemaud, Thomas, 2018. Colonization history of the western corn rootworm (*Diabrotica virgifera virgifera*) in North America: insights from random forest ABC using microsatellite data. Biological Invasions 20, 665–677.

Meihls, Lisa N, Higdon, Matthew L, Siegfried, Blair D, Miller, Nicholas J, Sappington, Thomas W, Ellersieck, Mark R, Spencer, Terence A, Hibbard, Bruce E, 2008. Increased survival of western corn rootworm on transgenic corn within three generations of on-plant greenhouse selection. Proc. Natl. Acad. Sci. USA. 105, 19177–19182.

Meinke, Lance J, Sappington, Thomas W, Onstad, David W, Guillemaud, Thomas, Miller, Nicholas J, Komáromi, Judit, Levay, Nora, Furlan, Lorenzo, Kiss, József, Toth, Ferenc, 2009. Western corn rootworm (*Diabrotica virgifera virgifera* LeConte) population dynamics. Agricultural and Forest Entomology 11, 29–46.

Mishra, R, Guo, Y, Kumar, P, Canton, P.E., Tavares, C.S., Banerjee, R, Kuwar, S, Bonning, B.C., 2021. Streamlined phage display library protocols for identification of insect gut binding peptides highlight peptide specificity. Current Research in Insect Science 1, 100012.

Moar, W., Khajuria, C., Pleau, M., Ilagan, O., Chen, M., Jiang, C., Price, P., McNulty, B., Clark, T., Head, G., 2017. Cry3Bb1-resistant western corn rootworm, *Diabrotica virgifera virgifera* (LeConte) does not exhibit cross-resistance to DvSnf7 dsRNA. PLoS ONE 12, e0169175.

Moellenbeck, D.J., Peters, M.L., Bing, J.W., Rouse, J.R., Higgins, L.S., Sims, L., Nevshemal, T., Marshall, L., Ellis, R.T., Bystrak, P.G., Lang, B.A., Stewart, J.L., Kouba, K., Sondag, V., Gustafson, V., Nour, K., Xu, D., Swenson, J., Zhang, J., Czapla, T., Schwab, G., Jayne, S., Stockhoff, B.A., Narva, K., Schnepf, H.E., Stelman, S.J., Poutre, C., Koziel, M., Duck, N., 2001. Insecticidal proteins from *Bacillus thuringiensis* protect corn from corn rootworms. Nat. Biotechnol. 19, 668–672.

Niu, X., Kassa, A., Hasler, J., Griffin, S., Perez-Ortega, C., Procyk, L., Zhang, J., Kapka-Kitzman, D.M., Nelson, M.E., Lu, A., 2020. Functional validation of DvABCB1 as a receptor of Cry3 toxins in western corn rootworm, *Diabrotica virgifera virgifera*. Sci. Rep. 10, 15830.

Pacheco, S., Gomez, I., Arenas, I., Saab-Rincon, G., Rodriguez-Almazan, C., Gill, S.S., Bravo, A., Soberon, M., 2009. Domain II loop 3 of *Bacillus thuringiensis* Cry1Ab toxin is involved in a "ping pong" binding mechanism with *Manduca sexta* aminopeptidase-N and cadherin receptors. J. Biol. Chem. 284, 32750–32757.

Park, Y., Abdullah, M.A., Taylor, M.D., Rahman, K., Adang, M.J., 2009. Enhancement of *Bacillus thuringiensis* Cry3Aa and Cry3Bb toxicities to coleopteran larvae by a toxin-binding fragment of an insect cadherin. Appl. Environ. Microbiol. 75, 3086–3092.

Park, Y., Hua, G., Ambati, S., Taylor, M., Adang, M.J., 2019. Binding and synergizing motif within coleopteran cadherin enhances Cry3Bb toxicity on the Colorado potato beetle and the lesser mealworm. Toxins 11 (7), 386. doi:10.3390/toxins11070386.

Pauchet, Y., Bretschneider, A., Augustin, S., Heckel, D.G., 2016. A P-glycoprotein is linked to resistance to the *Bacillus thuringiensis* Cry3Aa toxin in a leaf beetle. Toxins 8 (12), 362. doi:10.3390/toxins8120362.

Petzold-Maxwell, Jennifer L, Cibils-Stewart, Ximena, Wade French, B, Gassmann, Aaron J, 2012. Adaptation by western corn rootworm (Coleoptera: Chrysomelidae) to Bt maize: inheritance, fitness costs, and feeding preference. J. Econ. Entomol. 105, 1407–1418.

Pierleoni, A., Martelli, P.L., Casadio, R., 2008. PredGPI: a GPI-anchor predictor. BMC Bioinformatics 9, 392.

Price, Daniel RG, Gatehouse, John A, 2008. RNAi-mediated crop protection against insects. Trends Biotechnol 26, 393–400.

Sayed, A., Nekl, E.R., Siqueira, H.A., Wang, H.C., Ffrench-Constant, R.H., Bagley, M., Siegfried, B.D., 2007. A novel cadherin-like gene from western corn rootworm, *Diabrotica virgifera virgifera* (Coleoptera: Chrysomelidae), larval midgut tissue. Insect Mol. Biol. 16, 591–600.

Schrader, PM, Estes, RE, Tinsley, NA, Gassmann, AJ, Gray, ME, 2017. Evaluation of adult emergence and larval root injury for Cry3Bb1-resistant populations of the western corn rootworm. Journal of Applied Entomology 141, 41–52.

Shao, E., Lin, L., Chen, C., Chen, H., Zhuang, H., Wu, S., Sha, L., Guan, X., Huang, Z., 2016. Loop replacements with gut-binding peptides in Cry1Ab domain II enhanced toxicity against the brown planthopper, *Nilaparvata lugens* (Stal). Sci Rep 6, 20106.

Silva-Filha, M.H., Nielsen-Leroux, C., Charles, J.F., 1997. Binding kinetics of *Bacillus sphaericus* binary toxin to midgut brush-border membranes of *Anopheles* and *Culex* sp. mosquito larvae. Eur. J. Biochem. 247, 754–761.

Soberon, M., Pardo-Lopez, L., Lopez, I., Gomez, I., Tabashnik, B.E., Bravo, A., 2007. Engineering modified Bt toxins to counter insect resistance. Science 318, 1640–1642.

Spencer, Joseph L, Raghu, S, 2009. Refuge or reservoir? The potential impacts of the biofuel crop *Miscanthus* x *giganteus* on a major pest of maize. PLoS One 4 (12), e8336. doi:10.1371/journal.pone.0008336.

Tay, Wee Tek, Mahon, Rod J, Heckel, David G, Walsh, Thomas K, Downes, Sharon, James, William J, Lee, Sui-Fai, Reineke, Annette, Williams, Adam K, Gordon, Karl HJ, 2015. Insect resistance to *Bacillus thuringiensis* toxin Cry2Ab is conferred by mutations in an ABC transporter subfamily A protein. PLoS Genet 11 (11), e1005534. doi:10.1371/journal.pgen.1005534.

Tinsley, NA, Estes, RE, Gray, ME, 2013. Validation of a nested error component model to estimate damage caused by corn rootworm larvae. J. Appl. Entomol. 137, 161–169.

Urías-López, Mario A, Meinke, Lance J, 2001. Influence of western corn rootworm (Coleoptera: Chrysomelidae) larval injury on yield of different types of maize. J. Econ. Entomol. 94, 106–111.

Vaughn, T, Cavato, T, Brar, G, Coombe, T, DeGooyer, T, Ford, S, Goth, M, Howe, A, Johnson, S, Kolacz, K, Pilcher, C, Purcell, J, Romano, C, English, L, Pershing, J, 2005. A method of controlling corn rootworm feeding using a *Bacillus thuringiensis* protein expressed in transgenic maize. Crop Sci 45 (3), 931–938.

Vilchez, S., 2020. Making 3D-Cry toxin mutants: much more than a tool of understanding toxins mechanism of action. Toxins 12 (9), 600. doi:10.3390/toxins12090600.

Walters, F.S., deFontes, C.M., Hart, H., Warren, G.W., Chen, J.S., 2010. Lepidopteran-active variable-region sequence imparts coleopteran activity in eCry3.1Ab, an engineered *Bacillus thuringiensis* hybrid insecticidal protein. Appl. Environ. Microbiol. 76, 3082–3088.

Walters, F.S., Stacy, C.M., Lee, M.K., Palekar, N., Chen, J.S., 2008. An engineered chymotrypsin/cathepsin G site in domain I renders *Bacillus thuringiensis* Cry3A active against western corn rootworm larvae. Appl. Environ. Microbiol. 74, 367–374.

Wechsler, S, Smith, D, 2018. Has resistance taken root in U.S. corn fields? Demand for insect control. Am. J. Agric. Econ. 100, 1136–1150.

Willse, A., Flagel, L., Head, G., 2021. Estimation of Cry3Bb1 resistance allele frequency in field populations of western corn rootworm using a genetic marker. G3 (Bethesda) 11 (1), jkaa013. doi:10.1093/g3journal/jkaa013.

Wu, C., Chakrabarty, S., Jin, M., Liu, K., Xiao, Y., 2019. Insect ATP-binding cassette (ABC) transporters: roles in xenobiotic detoxification and Bt insecticidal activity. Int. J. Mol. Sci. 20 (11), 2829. doi:10.3390/ijms20112829.

Yin, Y., Flasinski, S., Moar, W., Bowen, D., Chay, C., Milligan, J., Kouadio, J.L., Pan, A., Werner, B., Buckman, K., Zhang, J., Mueller, G., Preftakes, C., Hibbard, B.E., Price, P., Roberts, J., 2020. A new *Bacillus thuringiensis* protein for western corn rootworm control. PLoS ONE 15, e0242791.

Yu, C.S., Cheng, C.W., Su, W.C., Chang, K.C., Huang, S.W., Hwang, J.K., Lu, C.H., 2014. CELLO2GO: a web server for protein subCELlular LOcalization prediction with functional gene ontology annotation. PLoS ONE 9, e99368.

Zhang, Q., Hua, G., Adang, M.J., 2017. Effects and mechanisms of *Bacillus thuringiensis* crystal toxins for mosquito larvae. Insect Sci 24, 714–729.

Zukoff, Sarah N, Ostlie, Kenneth R, Potter, Bruce, Meihls, Lisa N, Zukoff, Anthony L, French, Lee, Ellersieck, Mark R, Wade French, B, Hibbard, Bruce E, 2016. Multiple assays indicate varying levels of cross resistance in Cry3Bb1-selected field populations of the western corn rootworm to mCry3A, eCry3.1Ab, and Cry34/35Ab1. J. Econ. Entomol. 109, 1387–1398.